Polymer 50 (2009) 5508–5517

Contents lists available at ScienceDirect

Polymer

journal homepage: www.elsevier.com/locate/polymer

Deformation behaviour and mechanical properties of polypropylene processed by equal channel angular extrusion: Effects of back-pressure and extrusion velocity

R. Boulahia [a,b], J.M. Gloaguen [c], F. Zaïri [a,*], M. Naït-Abdelaziz [a], R. Seguela [c], T. Boukharouba [b], J.M. Lefebvre [c]

[a] Université Lille 1 Sciences et Technologies, Laboratoire de Mécanique de Lille (UMR CNRS 8107), Avenue P. Langevin, 59655 Villeneuve d'Ascq Cedex, France
[b] Laboratoire de Mécanique Avancée, USTHB, BP32 El-Alia Bab-Ezzouar, 16111 Alger, Algeria
[c] Université Lille 1 Sciences et Technologies, Laboratoire de Structure et Propriétés de l'Etat Solide (UMR CNRS 8008), Bâtiment C6, 59655 Villeneuve d'Ascq Cedex, France

ARTICLE INFO

Article history:
Received 28 August 2009
Accepted 18 September 2009
Available online 22 September 2009

Keywords:
Equal channel angular extrusion
Back-pressure
Extrusion velocity

ABSTRACT

Severe plastic deformation by equal channel angular extrusion (ECAE) is an ingenious deformation process used to modify texture and microstructure without reducing sample cross-section. The application of single ECAE pass to polypropylene (PP) was meticulously investigated at room temperature using a 90° die-angle tooling. The ECAE-induced deformation behaviour was examined in relation to the load versus ram-displacement curves. Depending on extrusion conditions, PP displayed various types of plastic flow. For ram velocities beyond 4.5 mm/min, severe shear bands consisting of successive translucent and opaque bands were observed, accompanied on the top surface by more or less pronounced periodic waves. Although the application of a back-pressure significantly reduced the wave and shear-banding phenomena, slightly inhomogeneous shear deformation was still observed. Shear bands were only suppressed by decreasing extrusion velocity. The strain-induced crystalline microstructure was investigated by X-ray scattering. Shear-banded samples exhibited a strong texturing of the (hk0) planes along the shear direction in the translucent bands whereas perfect crystalline isotropy appeared in the opaque bands. Application of back-pressure and/or reducing ram velocity resulted in uniform texturing along the extruded sample. Yet, texturing changed from single shear to twin-like shear orientation about the shear direction. Mechanical properties changes of the extruded samples due to back-pressure and extrusion velocity effects were analyzed via uniaxial tensile tests. The tensile samples displayed multiple strain localizations in shear-banded materials whereas quite homogeneous deformation appeared for non-banded ones. These effects were connected with the crystalline texturing. The results also revealed significant increase in the strain hardening after ECAE. Digital image correlation technique suitable for large deformation was used for determining the full-field strain of the tensile samples in relation to tensile strain and ECAE conditions.

1. Introduction

Equal channel angular extrusion (ECAE), a metal forming technique developed by Segal [1] in the beginning of the 1980s, has become the subject of considerable interest in the last few years for controlling microstructure via high plastic deformation. The method consists of extruding a sample through a die with two channels of equal cross-section (Fig. 1). In the crossing plane of the two channels, the sample is subjected to a large simple shear strain. Considering that the sample cross-section is not modified, multi-pass extrusion can be performed to perform extremely large plastic strains. The homogeneity of plastic strain field is a fundamental condition to ensure homogeneity of microstructure and mechanical properties. However, depending on the specific properties of the material, the tool geometry and the process parameters, the strain state can change from the expected homogeneous simple shear to a complex inhomogeneous strain field.

Uniaxial and biaxial drawings in the solid-state have been used for long to improve stiffness and strength of thermoplastic polymer fibres and films [2,3]. Various solid-state forming techniques such as forging [4], ram-extrusion [5], die-drawing [6], have also been developed for improving mechanical properties of polymer bulk pieces via large plastic deformations. However, ECAE is the only one process that preserves the sample shape.

* Corresponding author. Tel.: +33 3 287 674 60; fax: +33 3 287 673 01.
E-mail address: fahmi.zairi@polytech-lille.fr (F. Zaïri).

0032-3861/$ – see front matter © 2009 Elsevier Ltd. All rights reserved.
doi:10.1016/j.polymer.2009.09.050

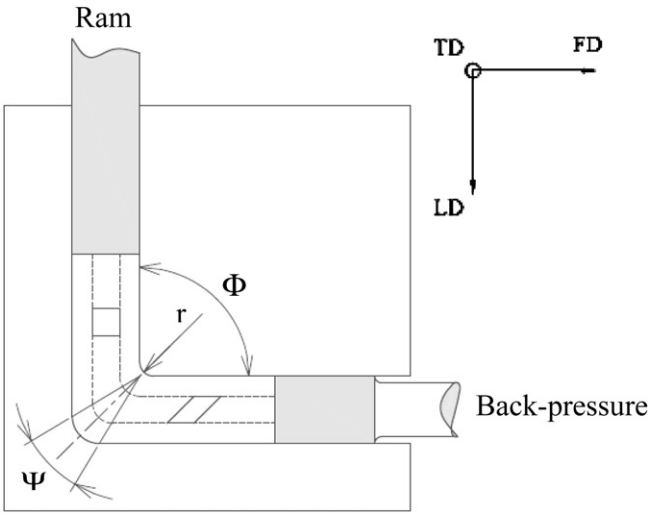

Fig. 1. Schematic illustration of a 90° ECAE die (flow direction: FD, load direction: LD, transverse direction: TD).

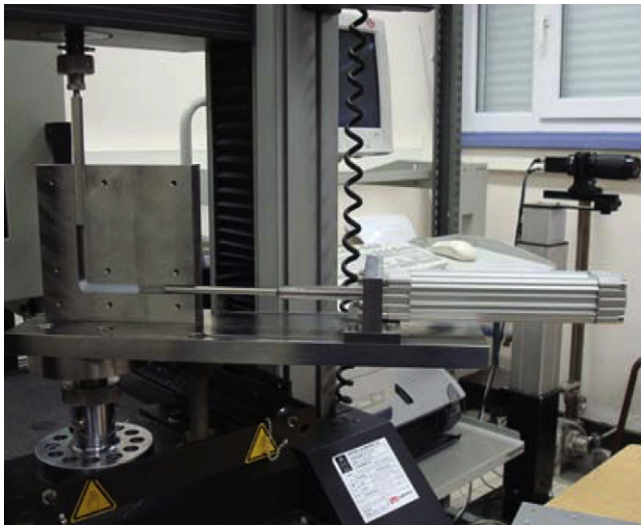

Fig. 2. Equipment used for ECAE with controlled back-pressure.

About 200 papers per year are published on the ECAE method (see ref. [7] and the references cited therein). However, relatively little attention has been focused so far on polymers processed by ECAE. The technique was applied to a polymer (low density polyethylene) for the first time by Sue and Li [8]. Since this first work, the ECAE was applied to several thermoplastic polymers such as polycarbonate, polymethylmethacrylate, high density polyethylene, polypropylene, semi-crystalline polyethylene-terephtalate, nylon-6, nylon-12 and polyacetal [8–27]. The morphological changes of polypropylene subjected to ECAE were examined by Campbell and Edward [9], and Phillips et al. [20]. However, neither the mechanics of the process nor the mechanical properties of the extruded material were examined. Campbell and Edward [9] used a constriction over the exit of the die and a "sacrificial sample" to create a back-pressure and to avoid the bending of the sample in the outer corner of the ECAE device. However, this technique does not allow to control the applied back-pressure and its actual role cannot be understood. Numerical simulations were recently conducted to examine the detailed effects of constitutive material behaviour, tool geometry, friction, extrusion velocity, extrusion temperature, number of extrusion sequences and processing route on polymer flow during ECAE [24–27].

In this paper, polypropylene samples were extruded using an experimental setup consisting of a 90° channel. Particular attention is paid to the analyses of the macroscopic flow behaviour during a single ECAE pass via the load–ram displacement measurements including the effect of back-pressure and extrusion velocity. The evolution of crystalline microstructure and mechanical properties of ECAE-processed samples is also meticulously investigated for understanding the plastic mechanisms of the process.

2. Material and experimental procedures

2.1. Material

The material used in this investigation is a polypropylene (PP) of weight–average molar weight of 180 kg/mol purchased from Goodfellow©. The material was supplied in the form of 10 mm thick compression-moulded plates.

2.2. ECAE experiments

ECAE experiments were conducted at room temperature (about 23 °C) and under constant ram speeds in the range of 0.45–45 mm/min. Samples were cut from the as-received PP plates along the same direction. The samples were 75 mm in length with square cross-sections 10 × 10 mm. The ECAE die was made of stainless steel. It is schematically given in Fig. 1. An internal angle Φ of 90° between the two channels, an outer corner angle Ψ of 10° and an inner radius r of 2 mm were adopted. The channels had cross-sectional dimensions of 10 × 10 mm. The ECAE tooling was adapted on an Instron© model 5800 screw testing machine (Fig. 2). The extrusion velocity and the back-pressure are kept constant during ECAE. Before each extrusion, the die was lubricated using silicone grease. Load–ram displacement data were recorded for each extrusion.

The plastic shear strain assigned to a sample as it passes through the ECAE die depends upon the two angles Φ and Ψ, and can be given by the following theoretical expression [28]:

$$\gamma = 2\cot\left(\frac{\Phi}{2}+\frac{\Psi}{2}\right)+\Psi\,\mathrm{cosec}\left(\frac{\Phi}{2}+\frac{\Psi}{2}\right) \quad (1)$$

In our case, Eq. (1) gives a plastic shear strain $\gamma = 1.9$. Note that this relationship assumes homogeneous shear deformation in the extruded sample.

2.3. Structural characterizations

Wide-angle X-ray scattering (WAXS) experiments were performed using the Ni-filtered Cu Kα radiation from a 2 kW Panalytical sealed tube operated on an INEL 2000 generator at 40 kV and 20 mA. The 2D-WAXS patterns recorded on a digital CCD camera from Photonic Science Ltd were corrected for background scattering.

2.4. Tensile tests

The tensile tests were conducted on the Instron© testing machine at room temperature under a constant cross-head speed 0.75 mm/min, *i.e.* a nominal strain rate of $10^{-3}\,s^{-1}$, using sample of gauge length 12.5 mm. Full-field strain measurements were achieved during tensile tests using digital image correlation (DIC) technique.

2.4.1. Tensile samples

Following extrusion, tensile samples were machined from the ECAE-processed pieces, the tensile axe being the FD axis. Three tensile samples (bottom, middle and top), which dimensions are given in Fig. 3, were cut from each extruded sample.

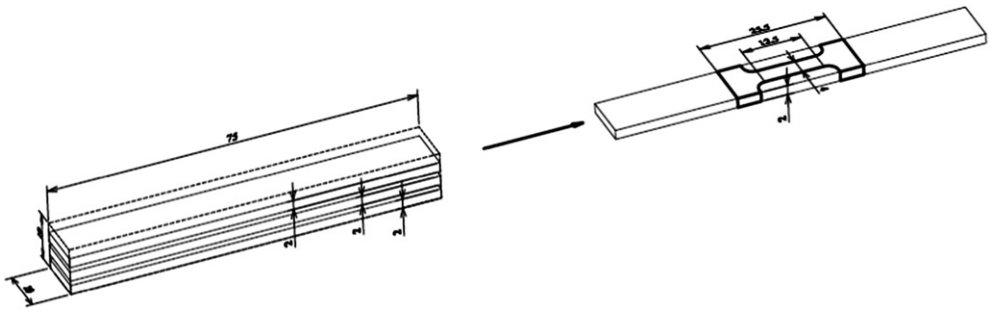

Fig. 3. Tensile samples after ECAE.

2.4.2. Strain measurements

DIC measurements require an artificial random speckle pattern which was generated by green dots sprayed on the surface of each sample. The random speckle pattern was applied so that speckles do not overlap. The studied zone was illuminated by a strong white light beam. The illuminated random speckle pattern was captured during the deformation by a digital CCD camera placed in front of the sample and at a distance of 0.5 m from the sample. The images of sample surface were recorded at a frequency of 2 Hz. DIC method is based upon comparing images of the sample surface in the undeformed (reference) and deformed states. By this way, a Lagrangian description is performed. A step of 10 images was used for the image correlation. The zone of interest was divided into small square sub-images of 64×64 pixels. The displacement vector was calculated using the corresponding sub-image pairs extracted from the reference and deformed states of the sample. By achieving the analysis on numerous sub-images, the full-field contours of displacement were obtained. The analysis was performed with Davis© software developed by Lavision©. The strain field was calculated from the obtained displacement field. A visual basic program was developed to calculate the true (logarithmic) strains from the full-field displacement data.

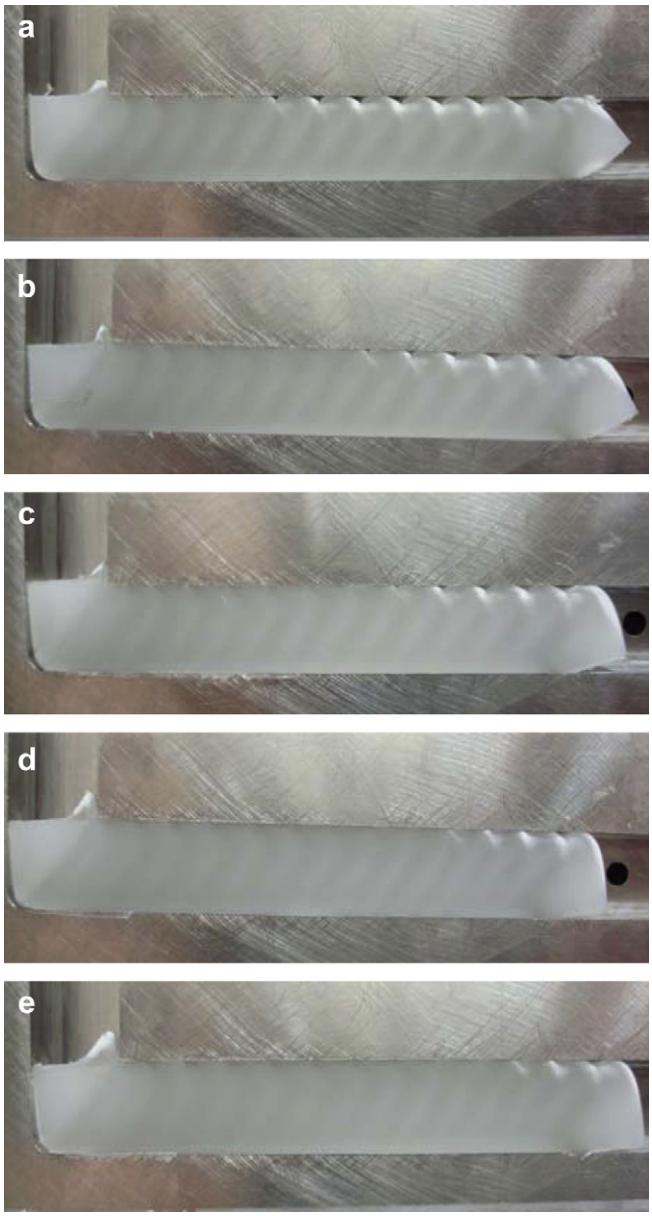

Fig. 4. Macrographs of PP samples after ECAE at a ram speed of 45 mm/min and different back-pressures: (a) 0 N, (b) 100 N, (c) 300 N, (d) 600 N, (e) 900 N.

3. Results and discussion

After the investigation of the extrusion behaviour of PP samples under various processing conditions, WAXS experiments are carried out for characterizing the structural evolution of the materials as a function of processing parameters. Then, the mechanical properties of extruded samples are presented and discussed.

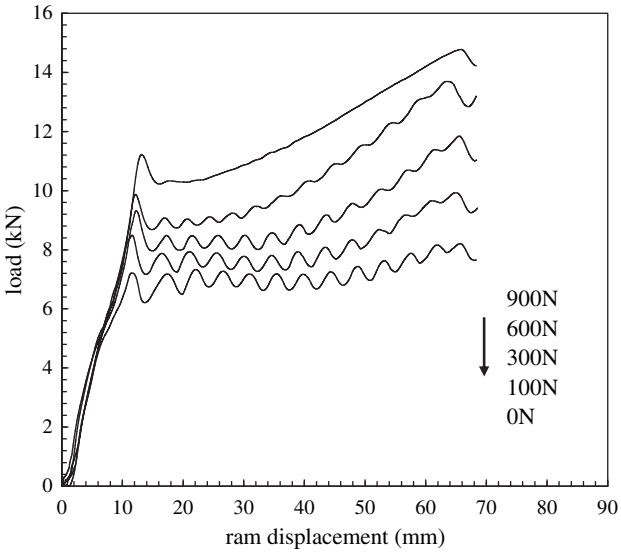

Fig. 5. Effect of back-pressure on load-ram displacement curves for ECAE of PP samples at a ram speed of 45 mm/min.

3.1. Macroscopic observations of ECAE-processed samples

3.1.1. Macroscopic effects of back-pressure

Fig. 4 presents the deformation behaviour of PP samples at the end of the ECAE operation performed at a ram speed of 45 mm/min. The strain pattern appears in a very particular manner. Without back-pressure (Fig. 4a), the sample does not fill up the outer corner of the die and exhibits a wavy shape on the top surface in the exit channel: the summit of the waves is in contact with the surface of the die whereas the bottom of the waves is not. This suggests a heterogeneous strain field in the bulk which is confirmed by the occurrence of dark grey and light grey alternated stripes inclined at about 45° from FD along the sample length. The dark and light stripes in reflected light are respectively translucent and opaque in transmitted light. This means that the former ones have undergone high shear that imparted severe deformation or destruction of the spherulitic structure whereas the later ones went undeformed through the transition zone of the ECAE, keeping intact the initial light-diffusing superstructure (see for comparison the undeformed part of the sample in the ECAE upstream channel in Fig. 4). Worth noticing is the study by Osawa et al. [29] of forged PP that displayed strong loss of turbidity as a result of strain-induced spherulitic size reduction. The fact that the sample does not fill up the outer corner of the tooling in the present study promotes the occurrence of a plastic instability accompanied with stress drop, as can be seen in Fig. 5. This kind of "stick-slip" phenomenon, never reported in previous ECAE studies on polymers, may be due to the combined effects of the specific visco-plastic behaviour of the material and the friction between the sample and the die, as a result of an unstable balance between the yield stress and the friction force. This interpretation borrows from previous studies regarding solid-state extrusion [30,31] and forging [4] of PP. The former study [30] reported stress oscillations and periodic surface irregularities of extruded PP under specific experimental conditions. The Russian authors developed a theoretical approach of solid-state extrusion accounting for viscoelastic turbulences.

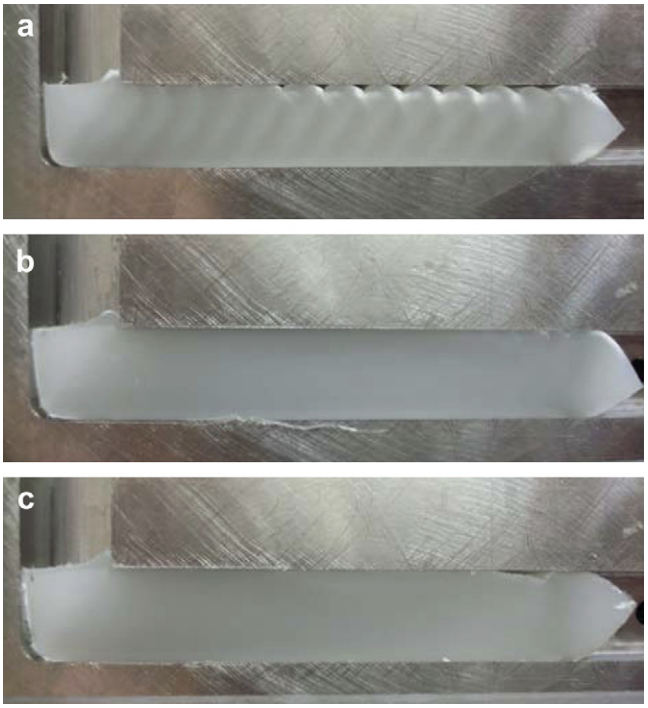

Fig. 6. Macrographs of PP samples after ECAE without back-pressure and different ram speeds: (a) 45 mm/min, (b) 4.5 mm/min, (c) 0.45 mm/min.

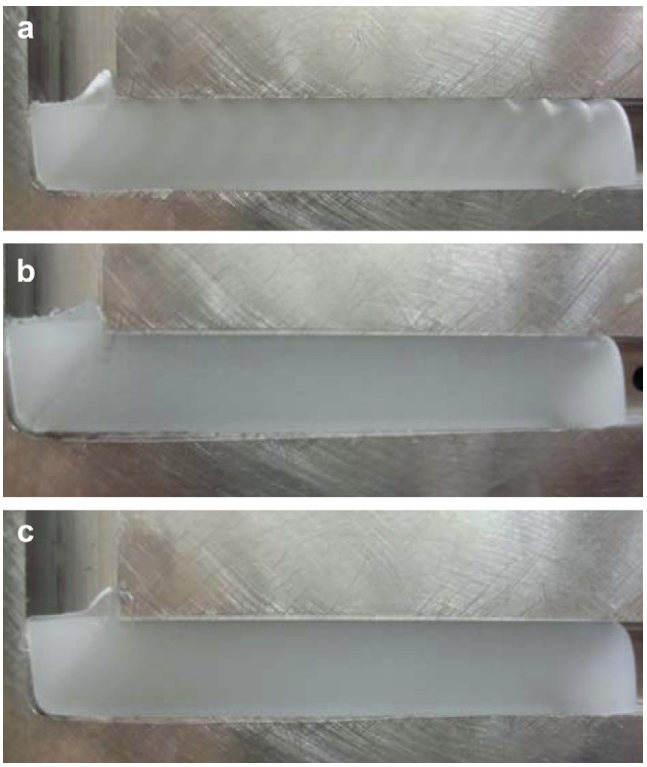

Fig. 7. Macrographs of PP samples after ECAE at a back-pressure of 900 N and different ram speeds: (a) 45 mm/min, (b) 4.5 mm/min, (c) 0.45 mm/min.

Kanamoto et al. [31] reported W-shape distortions of the flow profiles of high density polyethylene during the solid-state extrusion at high extrusion rates that were assigned to stick-slip [31]. Forging of PP has been also reported to involve a friction to stiction transition [4], the stiction process being responsible for yielding of the material at the surface only. In the present study, the curly shape of the summit of the waves without back-pressure (Fig. 4a) is relevant to plastic yielding confined within a limited surface layer of the material. This suggests that strong friction or stiction generates undeformed bands (light ones) with high plastic deformation close to the surface, whereas low

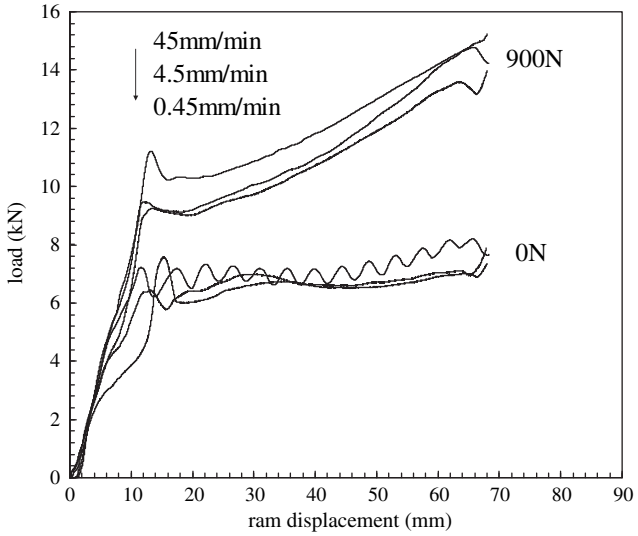

Fig. 8. Effect of ram speed on load–ram displacement curves for ECAE of PP samples at a back-pressure of 0 N and 900 N.

friction generates homogeneously sheared bands (dark ones) in the channel corner. The unstable balance between the yield stress and the friction force should be responsible for the both periodic stress oscillation and the periodic banding.

Die swell is another phenomenon that may generate periodic instabilities during the melt extrusion of polymers [32]. Viscoelastic relaxation of high elongation strains triggers transverse expansion of the material at the exit of the die. Die swell has been reported to occur in the case of the solid-state extrusion of low density polyethylene [33] that displays high viscoelastic capabilities owing to the large content of rubbery amorphous phase. No instabilities were yet mentioned by the authors. In the present study, the contribution of die swell is unlikely since the observed instabilities result in the opposite effect, *i.e.* the un-sheared bands do not fill up the channel cross-section (otherwise the sample cross-section is reduced with regard to the channel cross-section).

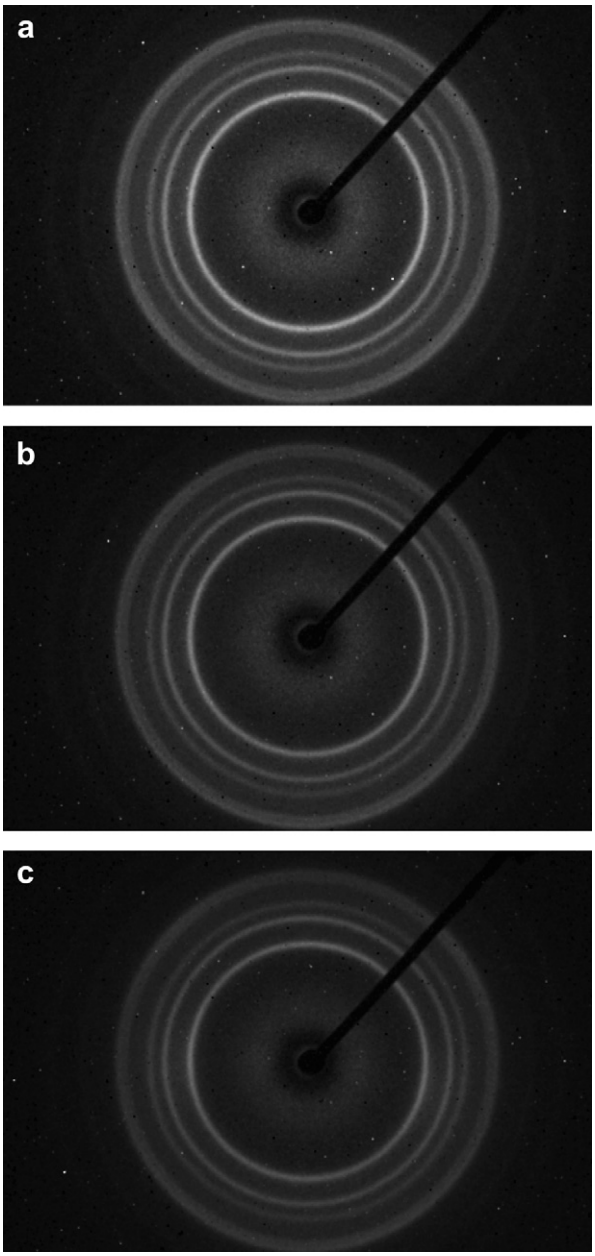

Fig. 9. 2D-WAXS patterns, viewing along FD axe, of PP after ECAE at a ram speed of 45 mm/min and without back-pressure: (a) top, (b) middle, (c) bottom.

The effect of back-pressure on the plastic flow instabilities is shown in Fig. 4. The application of back-pressure significantly contributes to reduce the gap between the sample and the outer corner of the die. The wave formation is concomitantly reduced and the alternating stripes tend to disappear with increasing back-pressure. However, a slight heterogeneity of the plastic strain field is still present along the sample length whatever the back-pressure level.

Fig. 5 shows the incidence of back-pressure on the load–ram displacement response. The magnitude of the load oscillations associated with the formation of shear bands decreases with the increase of back-pressure level while, in the meantime the overall load level increases due to both the yield stress sensitivity to hydrostatic pressure and the increasing friction of the material on the tooling.

3.1.2. Macroscopic effects of extrusion velocity

The effects of the loading rate on the deformation behaviour of PP samples at the end of the ECAE process are illustrated in Figs. 6 and 7 for two back-pressure values (0 N and 900 N, respectively). It is worth noting that, whatever the back-pressure value, under extrusion velocities of 4.5 and 0.45 mm/min, a quite uniform deformation field is obtained. In other words, the wave formation and shear bands described in the previous section vanish under these loading conditions.

This is again confirmed by the macroscopic response in terms of applied load–ram displacement curves as shown in Fig. 8. These curves do not exhibit oscillations as previously observed in Fig. 5. Moreover, without back-pressure, beyond a certain threshold, the curves exhibit a steady-state behaviour. When applying a back-pressure, the applied load continuously increases.

To obtain a uniform deformation field, it seems therefore better to proceed under reasonably low ram velocity and by applying a back-pressure in order to avoid the bending of the sample.

After these general macroscopic observations, the degree of microstructure heterogeneity and the induced mechanical properties generated in extruded samples are examined in the following sections.

3.2. Microscopic observations of ECAE-processed samples

The WAXS patterns recorded with the X-ray beam along the FD are quite isotropic, whatever the experimental conditions of the ECAE process. This is illustrated in Fig. 9 in the case of a slice taken from a dark stripe of the sample extruded at 45 mm/min without back-pressure, for three different positions from top to bottom of the slice, as sketched in Fig. 10. However, much different is the situation for the edge-view with the X-ray beam normal to the FD–LD plane. In the case of the higher ram velocity 45 mm/min and no back-pressure, Fig. 11 displays three 2D-patterns recorded from consecutive dark–light-dark stripes according to the sketch of

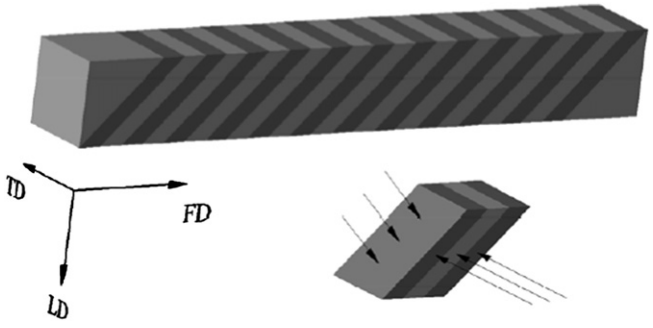

Fig. 10. Samples after ECAE for WAXS measurements.

Fig. 10. The middle light stripe looks roughly isotropic whereas the dark ones exhibit a strong diagonal reinforcement of the 3 first reflections. This is relevant to a preferred orientation of the (110), (040) and (130) planes containing the chain axis parallel to the shear direction. Indeed, pure shear of semi-crystalline polymers is well known to bring the chain-containing planes towards the shear direction, which is particularly the case of PP [34]. These findings corroborate the previous assumption that the light stripes arose from undeformed domains whereas the dark ones have undergone higher shear strain than the average value imposed by the ECAE device. The destruction of the spherulitic structure in the highly sheared bands reduces light scattering and makes them appear darker than the undeformed bands. It is worth noticing that the WAXS pattern is much similar to the one reported by Phillips et al. [20] for a high shear strain $\gamma = 3.1$, corroborating the above argument that the local shear strain is higher than that of the tooling. However, it is not believed that this is the fingerprint of a fibrillar structure since the WAXS pattern along the FD axe did not reveal any crystalline orientation (Fig. 9).

3.2.1. Microscopic effects of back-pressure

Applying a back-pressure of 900 N during the ECAE process at 45 mm/min results in the occurrence of scattering reinforcements on quadrant positions of the inner reflections as shown in Fig. 12. This reveals a double texturing of the (hk0) planes with a tilted orientation of the chain axis with respect to the ECAE shear plane. In the present case, the back-pressure not only turns the plastic deformation from highly heterogeneous to roughly homogeneous but also changes the plastic processes in the crystalline phase. The origin of the double texturing may be a double population of oriented crystallites as already reported from small-angle X-ray scattering studies regarding the ECAE of semi-crystalline polyethylene-terephthalate [12] and PP [20] as well. The mechanism of occurrence for this double population of crystallites was yet unexplained in either of the two studies. Alternatively, the double crystalline texturing could arise from a twinning mechanism, as already observed for PP under cold-rolling [35] or biaxial stretching [36]. In both instances, the driving force to the phenomenon might be the strong pressure-sensitivity of PP plastic yielding [37] that hinders the more compliant shear planes and thus provides opportunity for

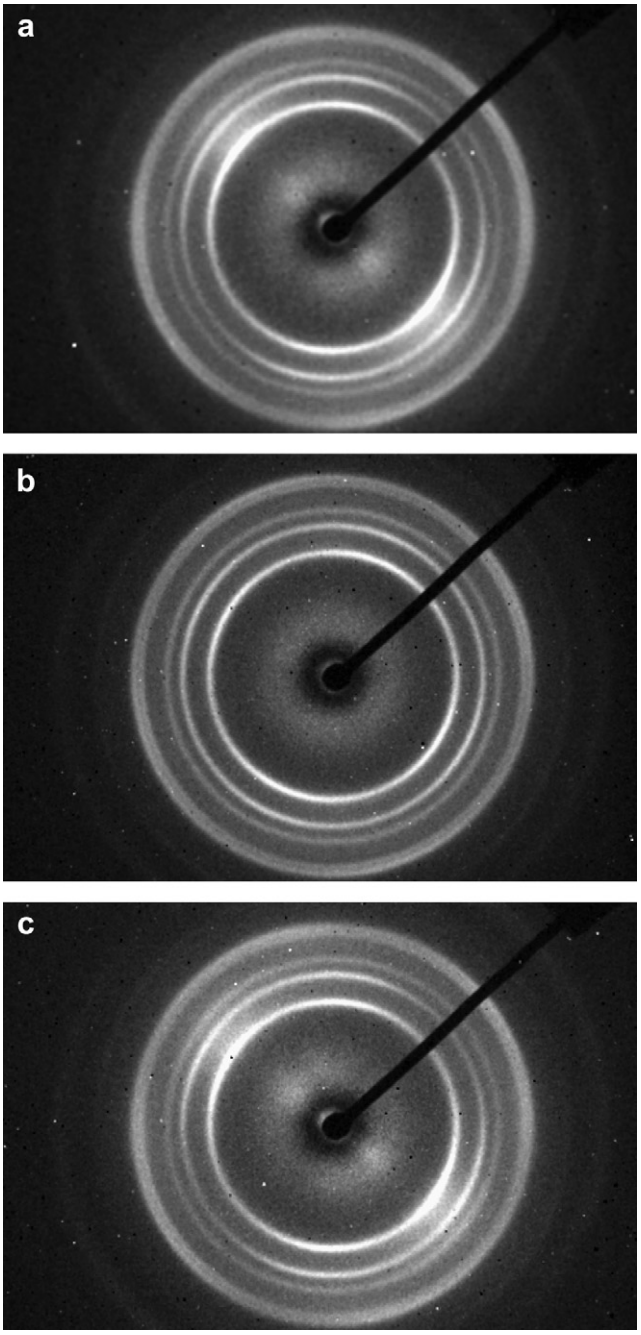

Fig. 11. 2D-WAXS patterns, viewing along TD axe, of PP after ECAE at a ram speed of 45 mm/min and without back-pressure: (a) dark stripe, (b) light stripe, (c) dark stripe (the shear direction is parallel to the beam stop arm).

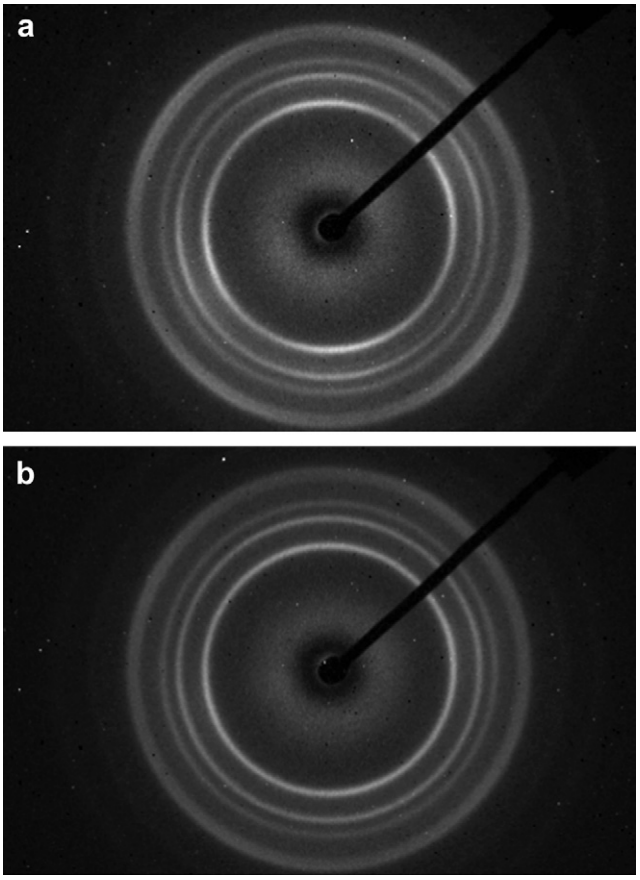

Fig. 12. 2D-WAXS patterns of PP after ECAE at a ram speed of 45 mm/min and a back-pressure of 900 N: (a) along TD axe, (b) along FD axe (the shear direction is parallel to the beam stop arm).

activation of less compliant ones. However, mechanical twinning is a process involving crystallographic shear normal to the chain axis in the crystal [38,39] that is inconsistent with the present findings. Otherwise, the tilting of the active crystallographic shear plane away from the maximum resolved shear stress plane due to the pressure-sensitivity may generate a double shear orientation.

3.2.2. Microscopic effects of extrusion velocity

It is worth studying the effect of low ram speed extrusion that also triggers homogeneous plastic deformation, even without back-pressure. The edge-view WAXS pattern of a sample extruded at 0.45 mm/min without back-pressure reported in Fig. 13 looks much similar to the one of Fig. 12, with quadrant (hk0) reflections roughly symmetric with regard to the shear plane of the EACE device.

To sum up, reducing the ram velocity by two decades has the same effect as applying a back-pressure of 900 N.

3.3. Mechanical properties of ECAE-processed samples

Tensile samples were cut off from the extruded material and mechanical tests were achieved to highlight the effect of back-pressure and extrusion velocity on the mechanical properties of extruded samples. Tests were performed at room temperature, with an initial strain rate of 10^{-3} s^{-1} and under constant cross-head speed condition. The measured load–displacement data were converted to average stress-strain curves.

Tensile behaviour of as-received PP sample is given in Fig. 14. The stress–strain curve exhibits a strain softening after yielding occurs. The stress decreases up to reach a quasi constant value as often reported for this material in the literature. A gradient in the mechanical properties can be clearly seen.

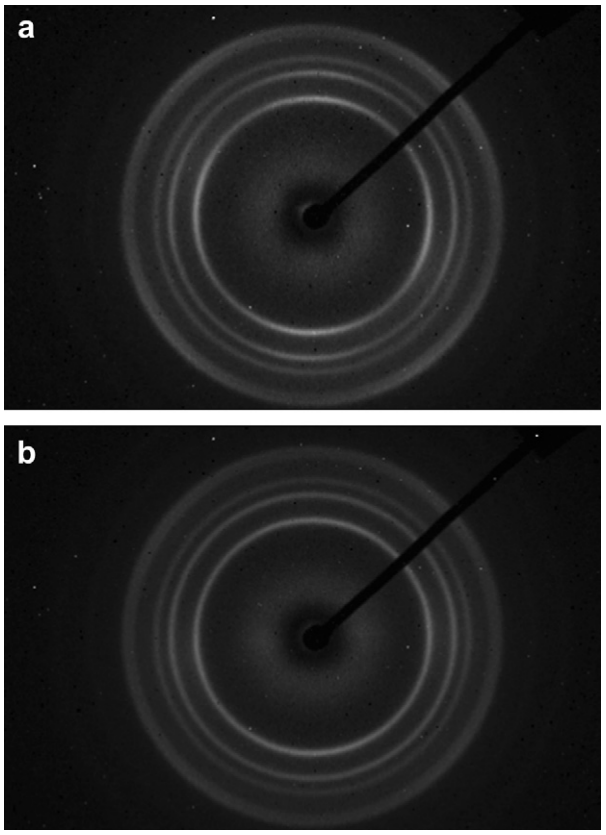

Fig. 13. 2D-WAXS patterns of PP after ECAE at a ram speed of 0.45 mm/min and without back-pressure: (a) along TD axe, (b) along FD axe (the shear direction is parallel to the beam stop arm).

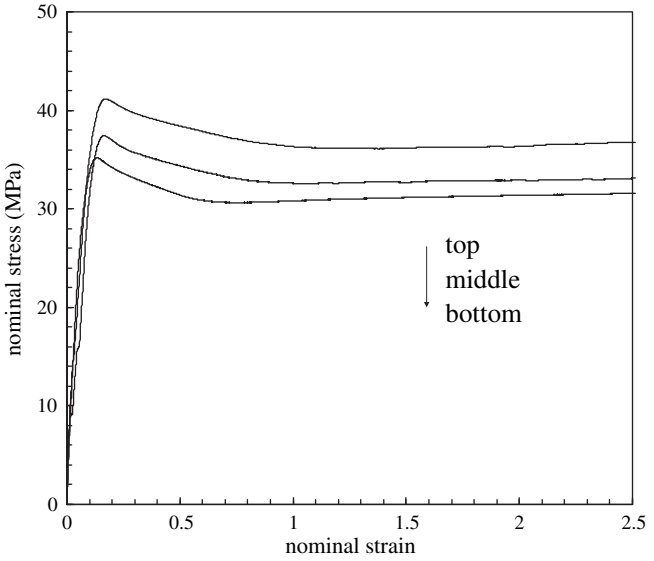

Fig. 14. Tensile stress–strain curves of an as-received PP sample.

3.3.1. Effects of back-pressure

The comparison of tensile behaviour of extruded samples at different back-pressure levels is shown in Fig. 15. The samples exhibit similar stress–strain behaviour. One can observe that the higher is the back-pressure value, the higher is the stress level. The yield stress of extruded samples is lower as compared to virgin samples. Furthermore, the stress–strain behaviour of extruded samples differs from that of virgin samples. Indeed, there is no stress softening but rather a linear hardening in all cases. This strain-hardening rate decreases with increase in back-pressure. This difference in the mechanical behaviour stems from textural modifications subsequent to back-pressure.

The inhomogeneity of mechanical properties in extruded samples was examined. Fig. 16 highlights this aspect for ECAE at a ram speed of 45 mm/min. The tensile properties of the top of the extruded sample without back-pressure were not evaluated because of the external waves. There is no appreciable difference between the

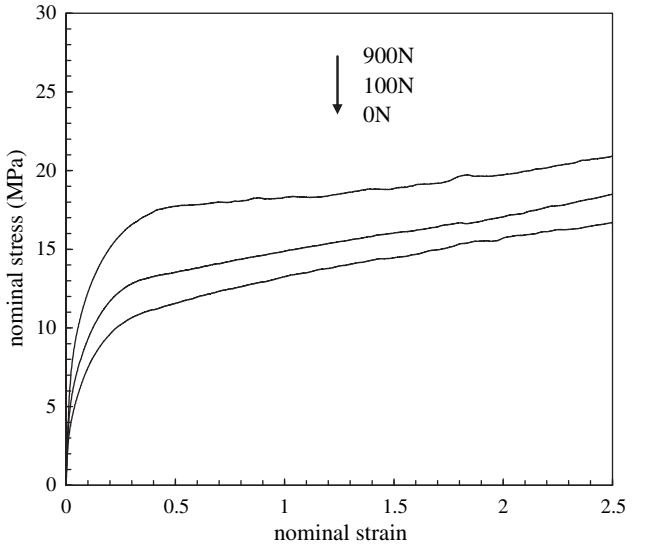

Fig. 15. Tensile stress-strain curves of PP samples after ECAE at a ram speed of 45 mm/min and different back-pressures.

middle and the top without back-pressure. When applying back-pressure, the mechanical properties are less uniform across the sample width, perhaps because of the edge effects. A strain hardening is observed in all cases and its rate changes across the sample width.

3.3.2. Effects of extrusion velocity

The effect of extrusion velocity on the stress versus strain curves (corresponding to samples extracted from the middle of the extruded material) is presented in Fig. 17. It is observed that there is a decrease in the yield stress as a function of extrusion velocity. The effect of extrusion velocity on the strain hardening can be clearly seen. Moreover, strain softening is also observed for the two lower velocities. In addition, when applying back-pressure, the differences observed on the global stress level are attenuated.

Extrusion velocity also acts on the homogeneity of the deformation after ECAE processing. As an example, two representative tensile samples are shown for a given cross-head displacement in

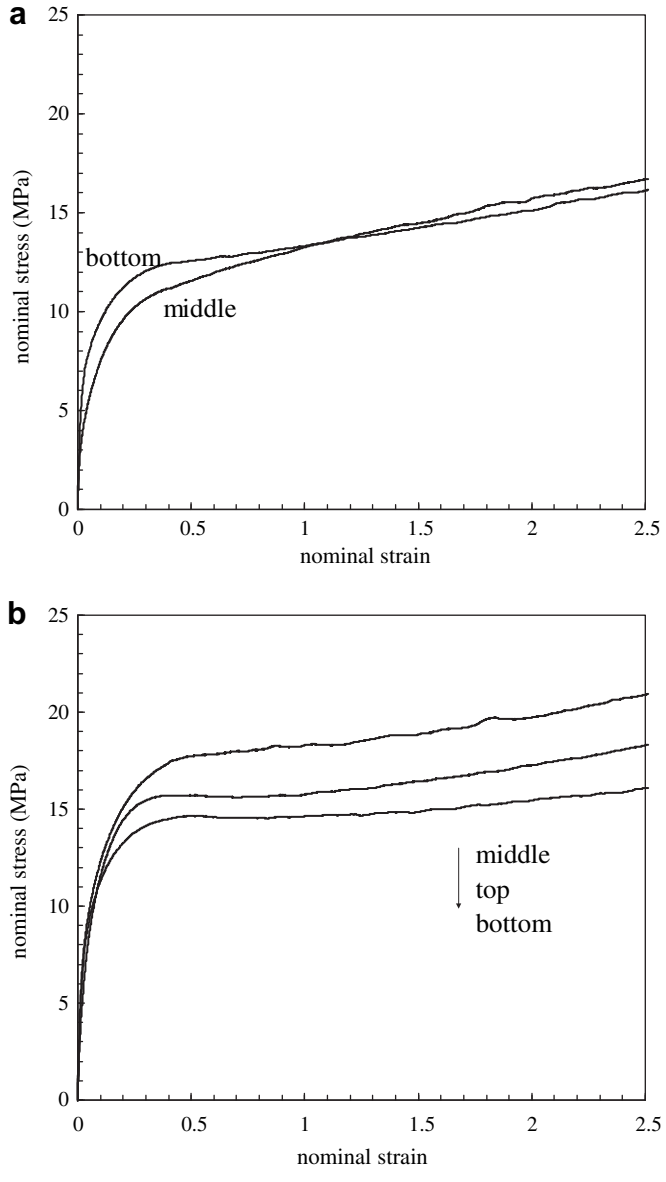

Fig. 16. Tensile stress–strain curves of PP samples after ECAE at a ram speed of 45 mm/min: (a) 0 N, (b) 900 N.

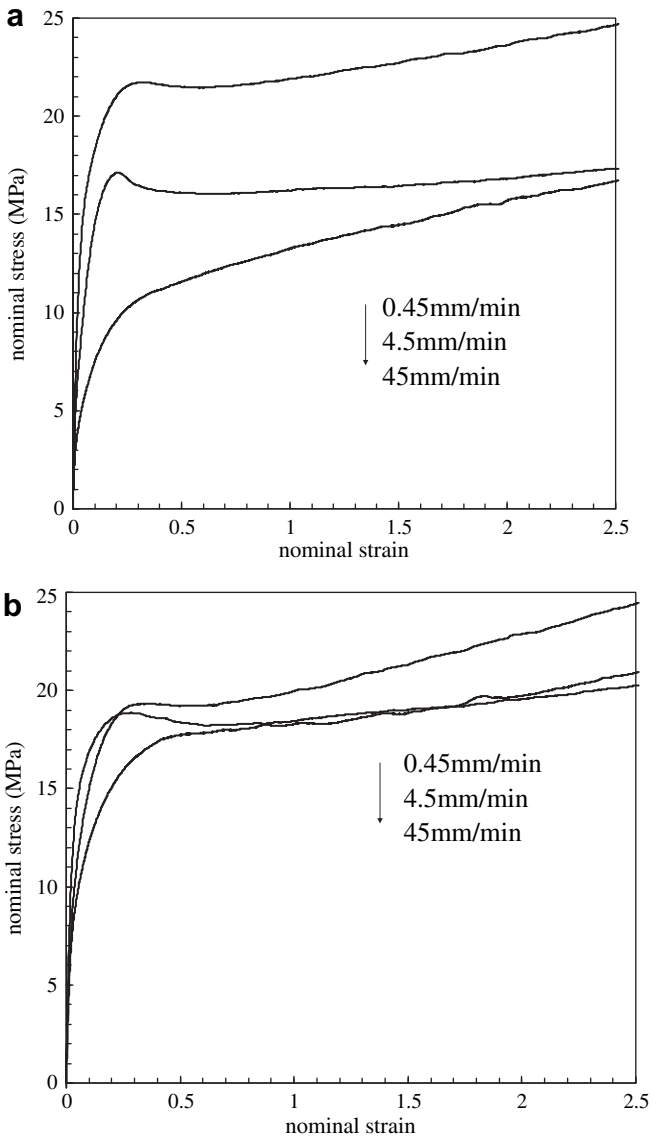

Fig. 17. Tensile stress–strain curves of PP samples after ECAE at different ram speeds: (a) 0 N, (b) 900 N.

Fig. 18. It can be clearly seen that the sample extruded at 4.5 mm/min presents a very diffused strain instability while multiple strain localizations occur in the sample extruded at 45 mm/min. These instabilities occur in regions undergoing high shear during extrusion. The specific crystallographic texturing of these sheared bands with their (hk0) planes tilted at roughly 45° from FD is indeed highly favourable to plastic shear when applying a tensile load along FD, owing to a maximum value of the resolved shear stress. It is noteworthy that, due to this specific crystallographic configuration, the tensile yield stress for the samples extruded at 45 mm/min is far below that of the other samples extruded at 4.5 and 0.45 mm/min (Fig. 17a). As strain increases beyond the yield point, the stress increase allows the undeformed regions to gradually proceed into plastic deformation process.

Further insight into the deformation behaviour is obtained by using the DIC method. Fig. 19 presents full-field contours of true axial strain at different stages of cross-head displacement u_y: 2.5, 6.25, 10 and 12.5 mm. The strain field is shown in colour level scale. True axial strain profiles along the length of samples are given in

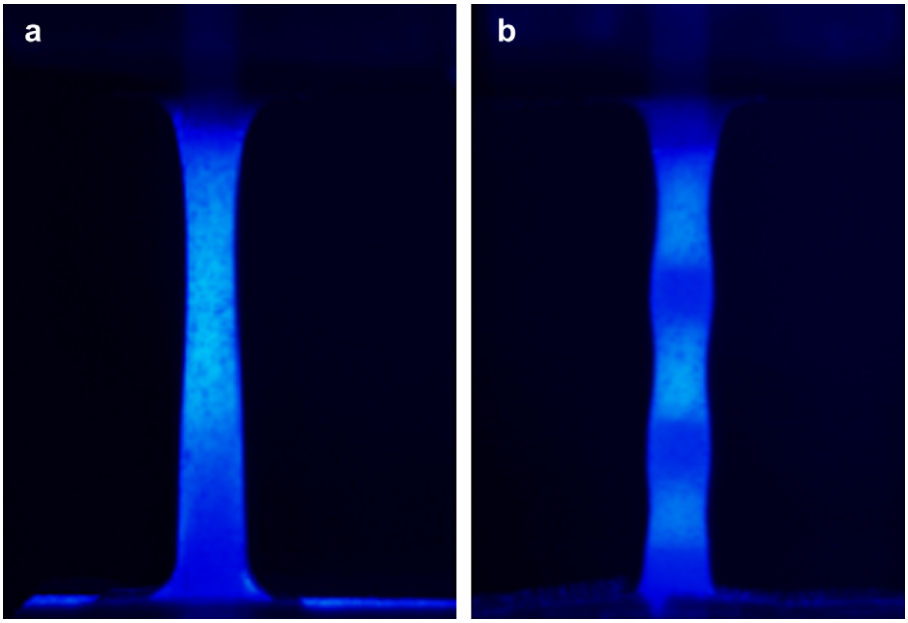

Fig. 18. PP tensile samples at a cross-head displacement of 12.5 mm after ECAE without back-pressure: (a) 4.5 mm/min, (b) 45 mm/min.

Fig. 20. The deformation is quite homogeneous before yielding and becomes inhomogeneous after strain instabilities occur. It can be observed from these figures that strain localization occurs at relative small cross-head displacements and increases with the increase of total displacement. The maximum local strain of the two examples is nearly comparable. However, the pattern of strain localization is completely different. Indeed, when considering multiple strain instabilities, the deformation remains nearly concentrated in the initiation zone while the instability is more diffused in the other case.

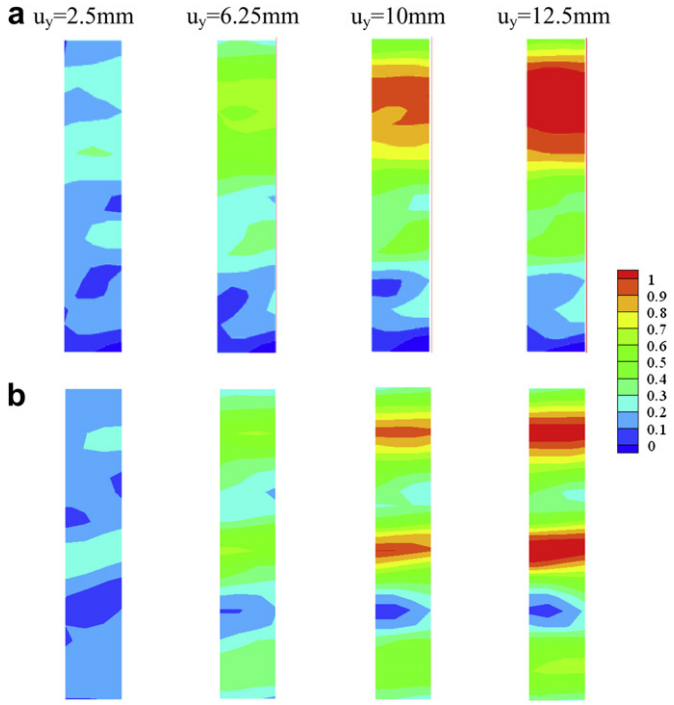

Fig. 19. Contour plots of true axial strain at different stages of cross-head displacement of a PP tensile sample after ECAE without back-pressure: (a) 4.5 mm/min, (b) 45 mm/min.

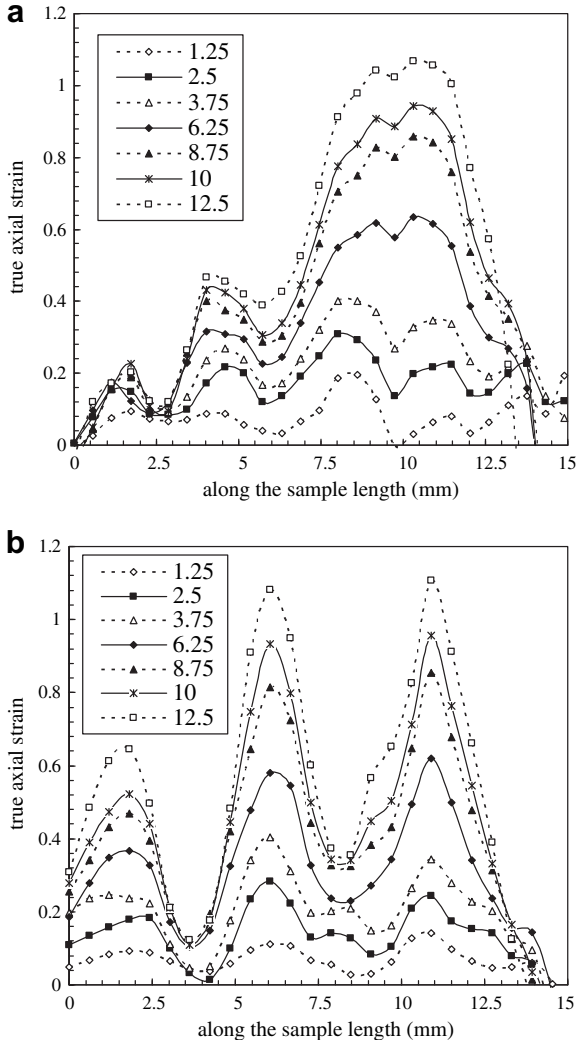

Fig. 20. True axial strain profiles along the length of a PP tensile sample after ECAE without back-pressure: (a) 4.5 mm/min, (b) 45 mm/min.

4. Conclusion

The ECAE of PP was conducted at room temperature under various extrusion velocities and back-pressure levels using a 90° die. It was shown that the application of back-pressure has a significant effect on the deformation homogeneity during ECAE. Very particular deformation behaviours were noted. Indeed, the inhomogeneity was externally manifested by periodic shear banding and periodic waves depending on the applied back-pressure level. Low extrusion velocities appear to provide benefits with regard to flow localization. Microscopic observations revealed important details of the deformation. Following the processing parameters different crystalline textures developed. The flow behaviour was examined by tensile testing of samples machined from ECAE samples. The virgin and extruded samples showed a high difference in strain hardening ability. The results show that multiple strain localizations occur during uniaxial tensile testing, revealing that extrusion velocity strongly acts on the deformation homogeneity of the extruded samples. Full-field strain was measured under tensile loading using an optical strain measuring technique based upon DIC which confirms these effects.

References

[1] Segal VM, Reznikov VI, Drobyshevskiy AE, Kopylov VI. Russ Metall 1981;1:99–105.
[2] Ward IM. Adv Polym Sci 1985;70:1–70.
[3] Osawa S, Zachariades AE, Saraf RF, Porter RS. J Macromol Sci, Rev Macromol Chem Phys 1997;C37:149–98.
[4] Saraf RF, Porter RS. J Rheology 1987;31:59–94.
[5] Zachariades AE, Mead WT, Porter RS. Chem Rev 1980;80:351–64.
[6] Coates PD, Ward IM. Polymer 1979;20:1553–60.
[7] Toth LS. Comp Mater Sci 2005;32:568–76.
[8] Sue HJ, Li CKY. J Mater Sci Lett 1998;17:853–6.
[9] Campbell B, Edward G. Plastics Rubb Comp 1999;28:467–75.
[10] Sue HJ, Dilan H, Li CKY. Polym Eng Sci 1999;39:2505–15.
[11] Li CKY, Xia ZY, Sue HJ. Polymer 2000;41:6285–93.
[12] Xia Z, Sue HJ, Rieker TP. Macromolecules 2000;33:8746–55.
[13] Xia Z, Sue HJ, Hsieh AJ. J Appl Polym Sci 2001;79:2060–6.
[14] Xia Z, Sue HJ, Hsieh AJ, Huang JWL. J Polym Sci Part B: Polym Phys 2001;39:1394–403.
[15] Creasy TS, Kang YS. J Therm Comp 2004;17:205–27.
[16] Xia Z, Hartwig T, Sue HJ. J Macromol Sci Part B 2005;43:385–403.
[17] Creasy TS, Kang YS. J Mater Process Technol 2005;160:90–8.
[18] Weon JI, Creasy TS, Sue HJ, Hsieh AJ. Polym Eng Sci 2005;45:314–24.
[19] Weon JI, Sue HJ. Polymer 2005;46:6325–34.
[20] Phillips A, Zhu PW, Edward G. Macromolecules 2006;39:5796–803.
[21] Wang ZG, Xia Z, Yu ZQ, Chen EQ, Sue HJ, Han CC, et al. Macromolecules 2006;39:2930–9.
[22] Al-Goussous S, Wu X, Yuan Q, Xia K. Mater Forum 2007;31:36–9.
[23] Ma J, Simon GP, Edward GH. Macromolecules 2008;41:409–20.
[24] Zaïri F, Aour B, Gloaguen JM, Naït-Abdelaziz M, Lefebvre JM. Comp Mater Sci 2006;38:202–16.
[25] Zaïri F, Aour B, Gloaguen JM, Naït-Abdelaziz M, Lefebvre JM. Scripta Mater 2007;56:105–8.
[26] Aour B, Zaïri F, Naït-Abdelaziz M, Gloaguen JM, Rahmani O, Lefebvre JM. Int J Mech Sci 2008;50:589–602.
[27] Zaïri F, Aour B, Gloaguen JM, Naït-Abdelaziz M, Lefebvre JM. Polym Eng Sci 2008;48:1015–21.
[28] Iwahashi Y, Wang J, Horita Z, Nemoto M, Langdon TG. Scripta Mater 1996;35:143–6.
[29] Osawa S, Mukai H, Ogawa T, Porter RS. J Appl Polym Sci 1998;68:1297–302.
[30] Krjutchkov AN, Dorfman IY, Prut EV, Enikolopyan NS. Polym Compos 1986;7:413–20.
[31] Kanamoto T, Zachariades AE, Porter RS. Polym J 1979;11:307–13.
[32] Graessley WW, Glasscock SD, Crawley RL. Trans Soc Rheology 1970;14:519–44.
[33] Benelhadjsaid C, Porter RS. J Appl Polym Sci 1985;30:741–53.
[34] G'Sell C, Dahoun A, Favier V, Hiver JM, Philippe MJ, Canova GR. Polym Eng Sci 1997;37:1702–11.
[35] Hibi S, Niwa T, Wang C, Kyu T, Lin J-S. Polym Eng Sci 1995;35:902–10.
[36] Bartczak Z, Martuscelli E. Polymer 1997;38:4139–49.
[37] Staniek E, Seguela R, Escaig B, François P. J Appl Polym Sci 1999;72:1241–7.
[38] Kiho H, Peterlin A, Geil PH. J Appl Phys 1964;35:1599–605.
[39] Allan P, Crellin EB, Bevis M. Philos Mag 1973;27:127–45.